

## Estimation of Surface Currents in the Adriatic Sea from Sequential Infrared Satellite Images

GIULIO NOTARSTEFANO, PIERRE-MARIE POULAIN, AND ELENA MAURI

*Istituto Nazionale di Oceanografia e di Geofisica Sperimentale (OGS), Trieste, Italy*

(Manuscript received 1 September 2006, in final form 17 May 2007)

### ABSTRACT

The maximum cross-correlation (MCC) technique is utilized to estimate the Adriatic Sea surface currents in regions characterized by strong horizontal temperature gradients using sequential pairs of sea surface temperature images from the Advanced Very High Resolution Radiometer data collected between September 2002 and December 2003. A variety of filtering techniques are used to eliminate erroneous MCC-derived currents resulting in velocity and direction estimates that are spatially coherent in most of the thermal features observed. The results are compared quantitatively to the currents measured by surface drifters and high-frequency coastal radars, operating simultaneously in the vicinity of the thermal structures considered. These comparisons show that surface MCC-derived velocities agree with the typical circulation pattern generally observed in the Adriatic basin. The MCC velocity estimates agree well with collocated and cotemporal drifter and radar measurements averaged on the time interval separating the pairs of images. Since the MCC method provides only estimates of surface currents when thermal features exist and are not covered by clouds, it is proposed that this technique be used preferably with other measurements of surface circulation (high-frequency coastal radars, drifters, etc.) to construct more accurate, more frequent, and more extended circulation maps for scientific and operational purposes in marginal seas such as the Adriatic.

### 1. Introduction

Estimating the ocean surface circulation, and in particular measuring the mesoscale surface currents, is a major goal in oceanography, but this requires a large amount of in situ data that have to be collected by ships, moored buoys, and/or by current meters. These data rarely yield a large geographic coverage and cannot provide a global observation of the ocean surface currents. Lagrangian drifters help to increase the geographical coverage but their sampling is usually not uniform in space and time.

The use of remote sensing techniques from the coast [high-frequency (HF) coastal radars] and from space (satellites) provides a more complete and frequent view of relatively large ocean areas. High-frequency coastal radars are successfully utilized to monitor and to map the surface circulation, but they are limited to within

100–200 km of the coast (Paduan and Graber 1997). Developments in the study of infrared satellite imagery have made it possible to estimate surface currents directly from sequential satellite images of sea surface temperature (SST) patterns. The first technique is based on a manual feature tracking and visual identification of surface thermal features. The displacements of the SST patterns are computed by observing the movements of selected features in pairs of sequential images (La Violette 1984; Vastano and Borders 1984; Vastano and Reid 1985; Vastano et al. 1985; Svejksky 1988). This methodology is rather subjective as it depends heavily on the SST features selected by the operator and on his/her ability to track them in subsequent images. The second technique, known as the maximum cross-correlation (MCC) technique, is more objective and involves very limited manual interaction to identify the surface thermal features. It was developed by Leese et al. (1971) for tracking clouds and was applied by Emery et al. (1986) to track oceanic mesoscale features. This procedure was also utilized to compute ice displacements in satellite visible images (Ninnes et al. 1986; Collins 1986; Collins and Emery 1988;

---

*Corresponding author address:* G. Notarstefano, Istituto Nazionale di Oceanografia e di Geofisica Sperimentale (OGS), Borgo Grotta Gigante, 42/c, 34010 Sgonico (Trieste), Italy.  
E-mail: gnotarstefano@ogs.trieste.it

Emery et al. 1991). In the MCC technique, the displacement of features between two satellite images is estimated by computing the cross correlation between sub-windows of the images. A basic and crucial factor to ensure accurate results is the use of well-navigated images because navigation errors can produce erroneous velocity estimates as reported by Breaker et al. (1994). To apply the MCC methodology, a primary element is the identification of SST features in sequential infrared satellite images.

Validation of the currents estimated by the MCC technique was performed by comparing the MCC results to velocity estimates obtained from surface drifters (Afanasyev et al. 2002), drogued drifters (Emery et al. 1986), and numerical models (Emery et al. 1992), to geostrophic currents (Emery et al. 1986; Afanasyev et al. 2002) derived from hydrographic data. In their study on the eastern Black Sea, Afanasyev et al. (2002) found a good agreement between the directions of the MCC currents, those measured by drifters (mean direction error of  $32^\circ$ ), and the directions of geostrophic currents (mean error of  $45^\circ$ ). An error of 11% was estimated when comparing the magnitudes of the MCC currents with the drifter results. Studies conducted by Emery et al. (1986) in the British Columbia coastal ocean revealed that MCC currents were consistent with both the velocities of drogued (5–10 m) drifters and with CTD-derived geostrophic current velocities. Emery et al. (1992) used a quasigeostrophic numerical model to validate the MCC technique in the Gulf Stream region. Surface currents simulated by the model compared well with those computed with the MCC technique applied to the passive tracer transported by the model currents when using 12 h or less as the time interval between the tracer images (the mean and standard deviation differences are about  $1 \text{ cm s}^{-1}$  using an 8-h time difference).

In this work, we present an application of the MCC technique to estimate the Adriatic Sea surface currents in regions characterized by strong horizontal temperature gradients, where thermal instability features often develop, using SST values from Advanced Very High Resolution Radiometer (AVHRR) data collected between September 2002 and December 2003 during the Dynamics of Localized Currents and Eddy Variability in the Adriatic (DOLCEVITA) program. Previous application of the MCC technique in the Adriatic area was made by Borzelli et al. (1999) and Alberotanza and Zandonella (2004).

Borzelli et al. (1999) used pairs of nighttime images separated by 24 h, near the end of August 1990, 1991, and 1992 to compute the surface velocity field in the central Adriatic Sea, an area characterized by a cold

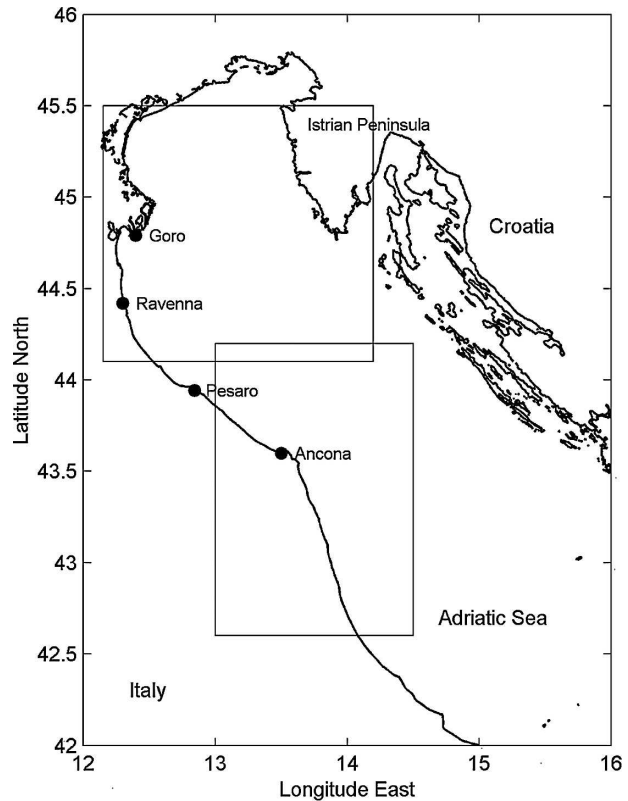


FIG. 1. Adriatic Sea and locations of the study areas and radar sites.

filament directed offshore from the Croatian coast and crossing the basin toward the Italian side. They found surface speeds ranging between  $10$  and  $20 \text{ cm s}^{-1}$ . Alberotanza and Zandonella (2004) estimated the sea surface circulation off the Italian coast (near Ancona) by applying the MCC to two pairs of SST images in September 1997, separated by about 3 and 10 h. They also used the results of HF coastal radars and found that the currents estimated by the 2 methodologies were similar (correlation coefficient near 0.75).

We have chosen to apply the MCC method to two areas of the Adriatic (Fig. 1), the northern subbasin and the area off the Monte Conero Promontory (near Ancona), where complex thermal structures and associated surface circulation features are prevailing. The northern Adriatic subbasin is characterized by the upper branch of the Eastern Adriatic Current (EAC) that flows northward along the Croatian coast, the Western Adriatic Current (WAC) running southward along the Italian side, and a cyclonic gyre in the northernmost part of the subbasin (Cushman-Roisin et al. 2001). This circulation pattern can sometimes be modified by an anticyclonic eddy located south of the Po River delta (Malanotte-Rizzoli and Bergamasco 1983; Hopkins et

al. 1999). The area along the Italian coast, near the Monte Conero Promontory, was studied in summer 2003 when the WAC reversed its typical southward circulation (Poulain et al. 2004a).

The MCC method is applied to several pairs of satellite SST images in the above-described regions. After the elimination of erroneous MCC currents using filtering techniques, the results are compared quantitatively to the currents measured by surface drifters operating simultaneously in the vicinity of the thermal structures considered and by HF coastal radars installed along the Italian coast south of the Po River delta.

The paper is organized as follows: section 2 provides a description of the satellite data used to apply the MCC technique and the drifter and HF radar data used for validation. In section 3, the MCC method and a brief account of the procedure limits are reported. The methodology adopted in this work and the filtering techniques utilized are described in section 4. Results of the analysis and comparison between the MCC-derived currents and drifter and radar data are summarized in section 5. Discussion and conclusions can be found in section 6.

## 2. Data

### a. AVHRR data

SST images were produced at Istituto Nazionale di Oceanografia e di Geofisica Sperimentale (OGS) in Trieste, Italy, using the AVHRR data transmitted by the National Oceanic and Atmospheric Administration (NOAA) polar orbiting satellites *NOAA-12*, *-14*, *-15*, *-16*, and *-17* and received by a TeraScan receiving station system. The data have a nominal resolution of  $\sim 1$  km and SST was estimated using the Multichannel Sea Surface Temperature (MCSST) algorithm described by McClain et al. (1985). In the processing, cloud identification was performed by using improved cloud masking tests, optimized for the Adriatic Sea area (Notarstefano et al. 2003). This masking procedure was improved to avoid considering areas of strong SST gradients as cloudy pixels, such as those along river plumes and fronts. Typically, a total of 10 images per day were produced; thus the time interval between successive images is relatively short (2–3 h).

We selected seven pairs of images in February 2003 and 1 pair in December 2003, with a time difference ranging between 8 and 12 h (Table 1) for the northern Adriatic (Fig. 1), and three pairs for the area off Ancona (covering the period from 17 to 19 July 2003) separated by about 8 h each. All images were manually navigated to reduce the error in georeferencing to

TABLE 1. Pairs of AVHRR SST images used for the MCC analysis.

Date and UTC	Satellite	Time separation (h:min)	Area of analysis
2 Feb 2003 1457	<i>NOAA-12</i>	6:33	Northern Adriatic
2 Feb 2003 2130	<i>NOAA-17</i>		
7 Feb 2003 0457	<i>NOAA-12</i>	7:52	Northern Adriatic
7 Feb 2003 1249	<i>NOAA-16</i>		
9 Feb 2003 1226	<i>NOAA-16</i>	8:06	Northern Adriatic
9 Feb 2003 2032	<i>NOAA-17</i>		
18 Feb 2003 1755	<i>NOAA-15</i>	12:16	Northern Adriatic
19 Feb 2003 0611	<i>NOAA-15</i>		
20 Feb 2003 1601	<i>NOAA-12</i>	10:07	Northern Adriatic
21 Feb 2003 0208	<i>NOAA-16</i>		
23 Feb 2003 1311	<i>NOAA-16</i>	12:24	Northern Adriatic
24 Feb 2003 0135	<i>NOAA-16</i>		
25 Feb 2003 0124	<i>NOAA-16</i>	11:25	Northern Adriatic
25 Feb 2003 1249	<i>NOAA-16</i>		
17 Jul 2003 0139	<i>NOAA-16</i>	8:14	Off Ancona
17 Jul 2003 0953	<i>NOAA-17</i>		
18 Jul 2003 0128	<i>NOAA-16</i>	8:02	Off Ancona
18 Jul 2003 0930	<i>NOAA-17</i>		
19 Jul 2003 1241	<i>NOAA-16</i>	7:47	Off Ancona
19 Jul 2003 2028	<i>NOAA-17</i>		
25 Dec 2003 1255	<i>NOAA-16</i>	7:37	Northern Adriatic
25 Dec 2003 2032	<i>NOAA-17</i>		

about one pixel ( $\sim 1$  km). The automatic navigation procedure (based on a TeraScan routine) usually provides a ground location accuracy of about 2 pixels.

### b. Drifter data

To compare MCC currents to in situ measurements, we used drifter data collected from September 2002 to December 2003 during the DOLCEVITA program. More than 100 drifter buoys (Poulain et al. 2003; Poulain and Barbanti 2003; Ursella et al. 2004, 2006) were deployed. Drifters were tracked by the Argos Data Location and Collection System (DCLS) carried by the NOAA polar orbiting satellites (Poulain et al. 2004b). Drifter positions are estimated from the Doppler shift caused by the relative motion between the drifter and the satellite. After editing to exclude outliers, the drifter position accuracy is 200–300 m. Some drifters were equipped with a global positioning system (GPS). For these drifters, GPS positions were recorded at hourly intervals. They were stored and transmitted during the satellite overpasses. The geographical location accuracy for the GPS drifters is within  $\pm 10$  m (Barbanti et al. 2005). Using the Argos system onboard two satellites (which is mostly the case for the DOLCEVITA drifters), positions are typically sampled 7 times per day (see Ursella et al. 2004), whereas GPS data are hourly.

### c. Radar data

HF coastal radars were operated in the northern Adriatic Sea starting in September 2002 as part of the DOLCEVITA program. Three Wellen Radar (WERA) HF radars were installed in Goro, Ravenna, and Pesaro, Italy (see locations in Fig. 1), to monitor the surface circulation patterns of the northern Adriatic basin between about 44° and 45°N. They were operated near 16 MHz in both beam-forming and direction-finding modes. For each radar, radial currents were obtained from the Doppler shift of Bragg lines in the spectrum data. Maps of radial currents were produced at intervals ranging between 20 min and 1 h. These radial maps were combined to produce hourly maps of the surface currents (bidimensional vectors) on a uniform grid with 5 km × 5 km spacing in longitude and latitude. These data were averaged in time with a 4-h-long running mean. More details on the radar data editing and smoothing can be found in Chavanne et al. (2007). For the time periods considered in this study, only the HF radar from the Goro and Pesaro sites is available. To assure accurate results, we restricted the data using the geometry with respect to the sites of Goro and Pesaro. In particular, we removed data locations whose azimuthal differences between the two sites are smaller than 70° and larger than 110°. In this way, we reduced the geometric error in the reconstruction of the radar signal and therefore the error in the determination of the velocity components.

## 3. MCC technique

### a. Definition

The MCC method computes the movement of thermal features between two sequential infrared images by searching the maximum cross correlation of the temperature patterns between a subwindow (herein named template window) of the first image and another one of the same size moved around a larger subwindow (herein named search window) of the second image (Ninnis et al. 1986; Emery et al. 1992). The size of the template window is chosen so as to contain enough features for tracking the structure of the current flow. Several studies have been conducted using this technique, and a template window size ranging between 20 and 40 km was generally used (Afanasyev et al. 2002; Barton 2002; Bowen et al. 2002; Emery et al. 1992; Kelly and Strub 1992; Tokmakian et al. 1990; Wilkin et al. 2002). The choice of the template window size is a fundamental parameter. Indeed, if the size is smaller than the SST features, it is difficult to find the same

features in the second image. Moreover, the correlation coefficients remain low and the MCC vectors can become erroneous. In contrast, if the size is too large with respect to the SST features, the resulting displacement vectors are smoothed out spatially. The size of the search window is specified in order to cover an area corresponding to the largest displacement expected for SST features, therefore the size of the search windows will change depending on the image time separation. The location of the window in the second image that corresponds to the maximum correlation with the “template window” in the first image represents the end point of the displacement originating at the center of the template window. The corresponding mean velocity is defined as the displacement divided by the time interval between the images. By moving the template window throughout the first image it is possible to generate a velocity map with a spatial resolution defined by the size of the window displacement.

### b. Limitations

In the MCC analysis, any variation of SST patterns is considered only due to horizontal surface advection. It is difficult to establish whether nonadvective mechanisms (mixing, heating, or cooling processes) or vertical motion (downwelling and upwelling events) are involved in the SST changes. By keeping the time interval between the two images shorter than 12 h it is more likely that physical processes related to diffusivity cannot strongly affect the SST patterns. Vertical motion and horizontally patchy heating or cooling events have to be considered sources of errors that could alter the SST patterns and it could happen that an MCC-derived velocity represents a heating/cooling event instead of a horizontal advection (Emery et al. 1986). Another problem can be that temperature changes caused by the use of different satellites can occur from one image to the other (Notarstefano et al. 2006).

Since temperature is generally not conserved in the upper ocean, in order to apply the MCC technique to a pair of SST images, Tokmakian et al. (1990) and Emery et al. (1992) suggest using a time interval of less than 12 h between the images to achieve the best velocity estimation and to minimize errors. For long time intervals (more than 12 h) MCC velocity vectors cannot show rotational motions of the circulation patterns, while for short time separations (3–5 h) the displacement is smaller, which makes it easier to detect translations in the rotational motion (Emery et al. 1986). The smallest velocity that can be resolved with 1 pixel displacement ( $\sim 1$  km) and a time separation of 1 h is  $27.7 \text{ cm s}^{-1}$ .

This decreases to  $2.3 \text{ cm s}^{-1}$  for 12 h. Another limitation of the MCC technique is the impossibility of detecting currents moving along surface temperature fronts (Emery et al. 1986).

#### 4. Methods

The choice of pairs of images to use for the analysis depends on various factors such as the presence of significant thermal structures, the percentage of cloud coverage, and in some cases, the availability of contemporaneous and collocated drifter/radar data used for validation.

The template window size we utilize in this work is  $25 \times 25$  pixels and the search window has such dimension as to include the maximal expected speed of  $\sim 1 \text{ m s}^{-1}$ . As an example, if the time difference between the images is 8 h, the size of the search window is  $83 \times 83$  pixels. The template is moved throughout the SST image with steps of two pixels. Computation of the cross correlation requires that all values in the windows are used. Since cloud covered pixels are flagged out in the image processing, correlation is calculated ignoring these values. Template windows with more than 40% of masked pixels are not used to ensure robust statistical results. Moreover, template windows within which the standard deviation of the SST is less than  $0.4^\circ\text{C}$  are discarded because they are considered to lack substantial thermal features.

A further step is to filter the MCC velocity vectors to eliminate erroneous estimations. Faulty vectors can be produced, as previously mentioned, because of the nonadvective motion processes that can cause the SST changes and when the MCC analysis is strongly affected by masked cloudy pixels and land.

##### a. Filtering the MCC-derived vectors

In this work we partially applied the filtering technique proposed by Barton (2002). The first filter consists of setting a correlation coefficient cutoff level, below which MCC vectors are rejected. Thermal features that are horizontally advected can modify their patterns due to vertical motion and heat diffusion. Therefore, the cross-correlation coefficient between the template and the window of the same size within the search window is expected to be always less than one. A maximum cutoff value of 0.8 is used in our analysis.

The second filter is based on the reciprocal technique, according to which displacement vectors are compared to their reciprocal. The couple of images are swapped and the template window is now in the sec-

ond image, centered at the end of the original MCC vector, while the “search window” is now in the first image. The selected reciprocal vector is the one corresponding to the maximum cross-correlation coefficient. Vectors pass the test if the end of the reciprocal vector is within three pixels of the original starting location, both in the north–south and east–west directions.

The third filter is the nearest neighbor comparison, based on the assumption that currents are broad features with some continuity in speed and direction (Barton 2002). Thus, neighboring vectors must respect certain conditions to pass this filter and to be considered good vectors. Following Barton (2002), a good vector must have an amplitude ranging between 0.5 and 2 times that of neighboring vectors and a relative direction within  $50^\circ$ . Since an MCC vector can have a minimum of zero and a maximum of eight neighbors, it passes the nearest neighbor filter if it respects the following conditions:

- a vector with two or three neighbors must agree with two of these neighbors;
- a vector with four or five neighbors must agree with three of these neighbors;
- a vector with six or seven neighbors must agree with four of these neighbors;
- a vector with eight neighbors must agree with five of these neighbors.

The fourth filter eliminates vectors if the distance between the center of the template window and the location of the SST gradient maximum is larger than  $3/8$  of the template window diagonal. In this way, we constrain the MCC vectors to be located close to the corresponding tracked thermal feature. In addition, vectors corresponding to displacements of the same order of magnitude as the image spatial resolution ( $\sim 1 \text{ km}$ ) are removed.

Finally, it was required that a few vectors be manually removed at the end of the filtering process, because they were distinctly erroneous. In particular, we rejected three vectors produced from the MCC analysis of the image pairs on 17 July 2003 (off the Monte Conero Promontory area).

##### b. Drifter trajectories and HF radar velocities used to compare with MCC-derived vectors

To validate the MCC-inferred surface currents, we compare vectors produced by this technique with those computed from the drifter trajectories. The drifter positions were interpolated at the times of the two images

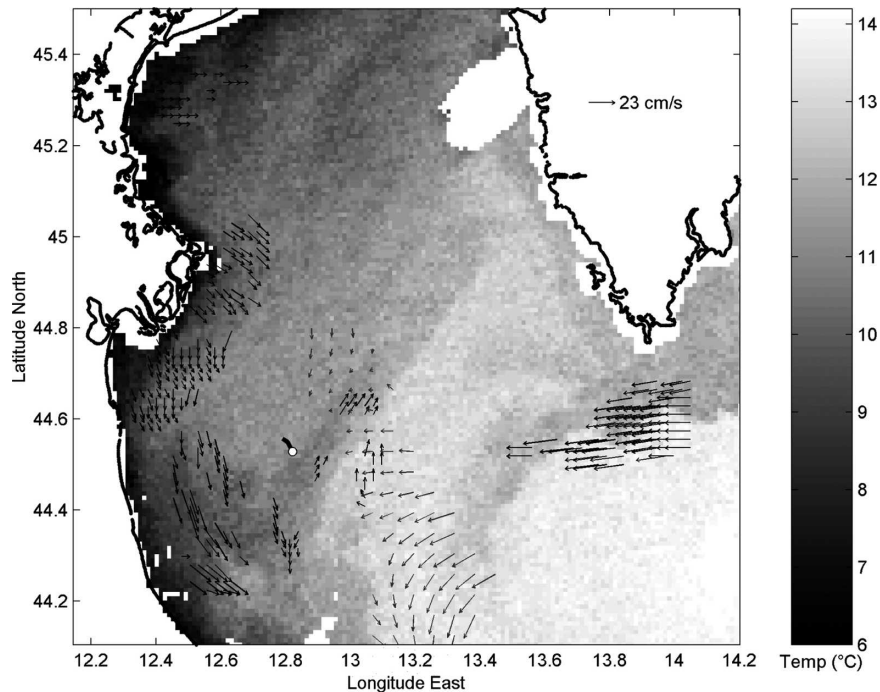


FIG. 2. AVHRR SST image for 1255 UTC 25 Dec 2003 (*NOAA-16*) with superimposed MCC-derived velocity vectors (black arrows), drifter trajectory segments over the same time interval (black segments with a white circle at the last position), and radar mean surface current vectors (gray arrows). Drifters that are used for comparison have a black circle at the last position. Land- and cloud-masked pixels are shown in white. The gray color scale is set to enhance the thermal features. Temperature is in degrees Celsius.

and the middle position was defined. The distance between this point and the middle position of the MCC displacement vector (the mean of the start and end positions) was computed. The comparison was made when this distance is at a minimum and less than 5 km. The mean drifter velocity was estimated by differencing the drifter positions interpolated at the image times, divided by the time interval between the two images.

The validation was also done using hourly radar measurements averaged over the time interval separating the pair of images. The comparison analysis was then executed following the same procedure explained above for the drifters.

## 5. Results

### a. Northern Adriatic

Eight pairs of images are used to describe the surface circulation pattern of the northern part of the Adriatic basin. A pair of images was acquired on 25 December 2003 (Fig. 2) and seven pairs during February 2003 (Figs. 3–9). Between 18 and 25 February, they are char-

acterized by the cold plume of the Po River extending south of the Po mouth and developing in the northeastern direction. The SST pattern is also dominated by the cold WAC, along the Italian coast. The warmer surface water pool, south of the tip of the Istrian Peninsula, flows westward and approaches the WAC. Instability features are striking on the thermal front separating the cold (to the north) and warm (to the south) waters.

The directions of the surface currents estimated by the MCC method are consistent with the typical circulation pattern observed in the northern Adriatic subbasin. They show the anticlockwise rotation of the warm feature south of the Istrian Peninsula and the northeastward propagation of the cold plume that is part of the northernmost cyclonic gyre of the basin (Cushman-Roisin et al. 2001; Lee et al. 2005). Vectors are spatially coherent over these thermal features exhibiting typical speeds of about  $10\text{--}20\text{ cm s}^{-1}$  (over the cold tongue and in the thermal front rooted off the Istrian Peninsula). Along the Italian coast, in some images (Figs. 2, 4, 5, 9), the MCC vectors indicate the usual southward flow of the WAC. MCC vectors located north of the Po River mouth show the southward flow along the Italian coast

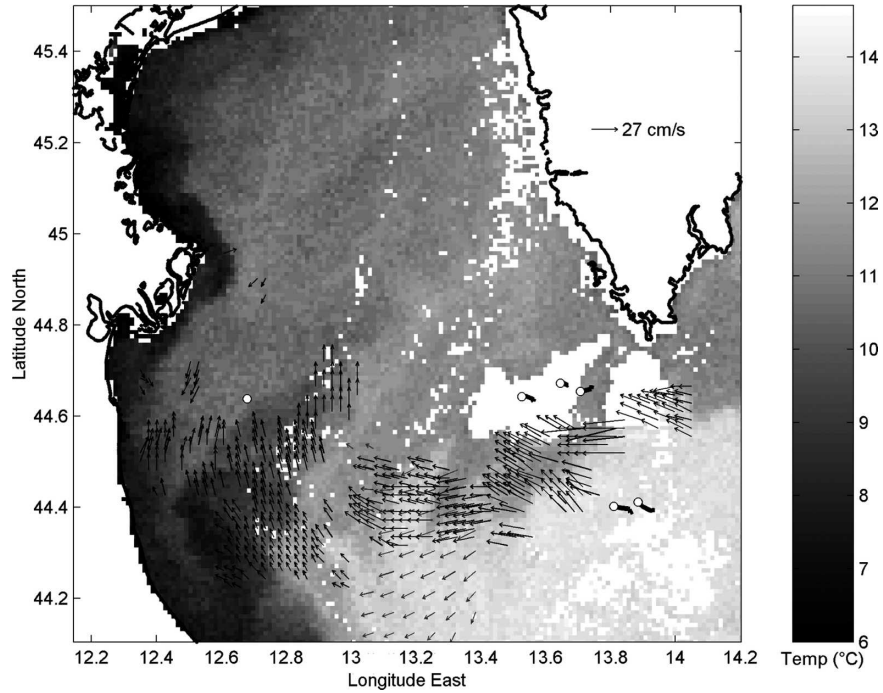


FIG. 3. Same as Fig. 2, but for 1457 UTC 2 Feb 2003 (NOAA-I2).

that is part of the northern cyclonic circulation. In some areas (see area south of Istria Peninsula on 2 February; Fig. 3) velocity vectors are less spatially coherent, probably due to the persistent cloud coverage that affects

the MCC analysis. However, the majority of the vectors agree with the circulation generally observed in this portion of the northern basin.

Validation statistics, including the number of vector

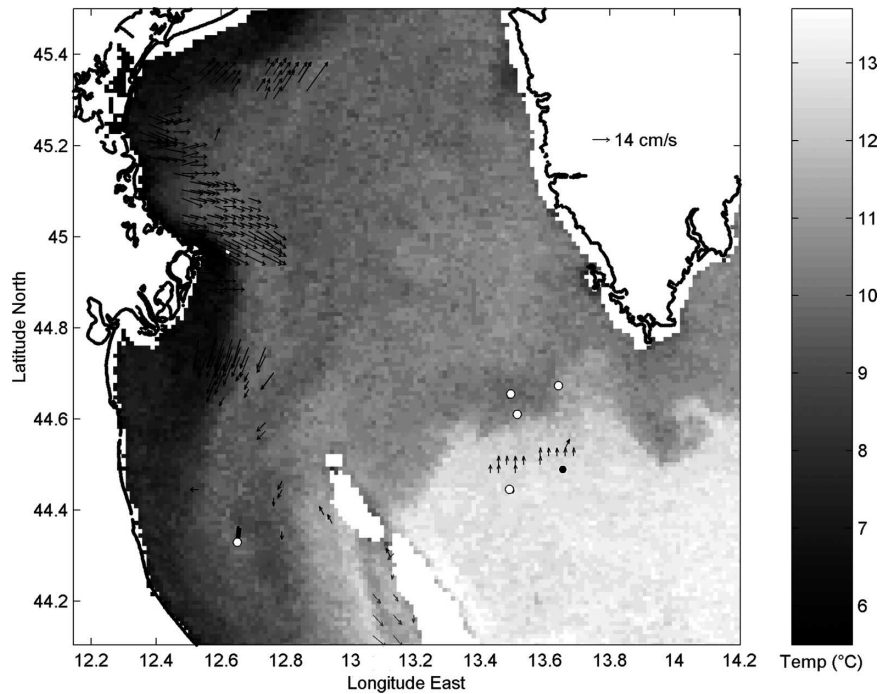


FIG. 4. Same as Fig. 2, but for 0457 UTC 7 Feb 2003 (NOAA-I2).

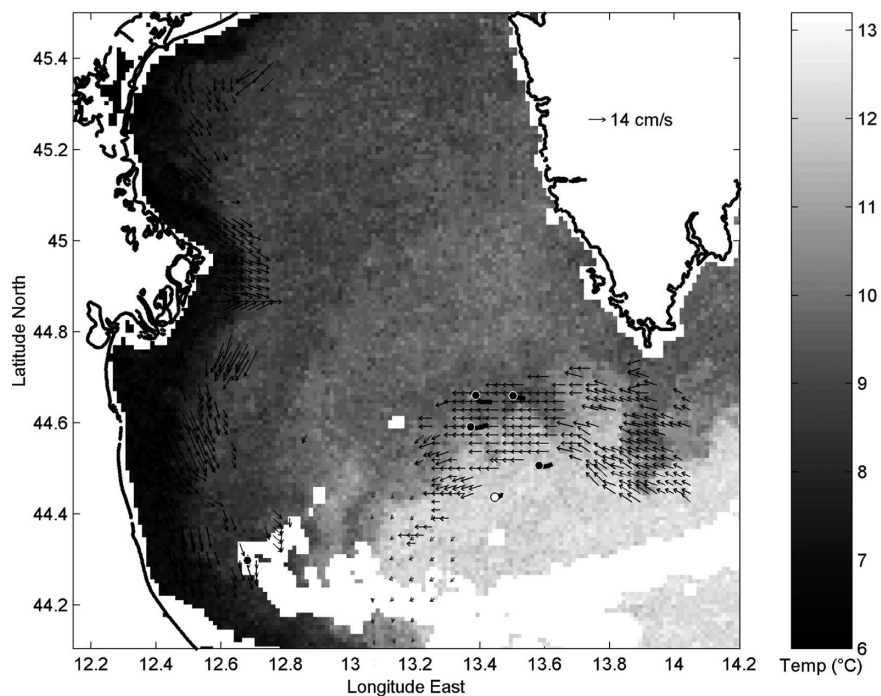


FIG. 5. Same as Fig. 2, but for 1226 UTC 9 Feb 2003 (NOAA-I6).

pairs, the mean, and the standard deviation of the velocity differences in both the zonal ( $u$ ) and meridional ( $v$ ) directions, are listed in Tables 2 and 3 for the comparison with drifter and radar data, respectively. The

difference is defined as the drifter (radar) velocity minus the MCC estimate.

The pair of images on 9 February (Fig. 5) provides the best validation result using drifter values:

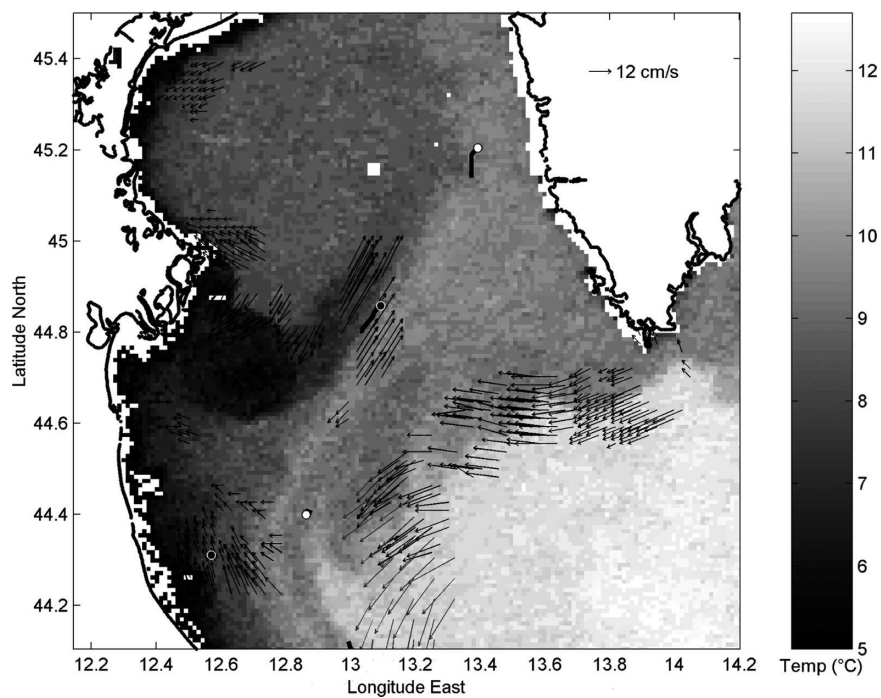


FIG. 6. Same as Fig. 2, but for 1755 UTC 18 Feb 2003 (NOAA-I5).



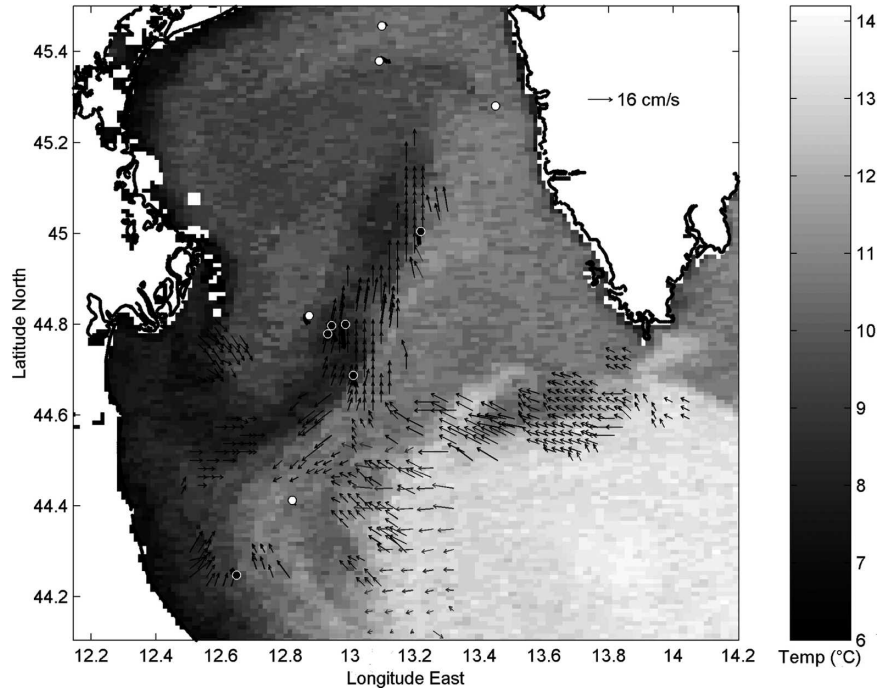


FIG. 7. Same as Fig. 2, but for 1601 UTC 20 Feb 2003 (NOAA-12).

the mean difference of the zonal (meridional) velocity component is  $-1.6 \pm 1.7$  ( $1.8 \pm 3.3$ )  $\text{cm s}^{-1}$ . The best mean difference of  $4.1 \pm 4.2$  ( $0.6 \pm 1.7$ )  $\text{cm s}^{-1}$ , using radar data, in the zonal (meridional) direction was found by applying the MCC technique

to the pair of images on 23–24 February (Fig. 8). On the contrary, there is a weaker agreement for the pair of images on 25 December (Fig. 2) and on 17 July (Fig. 10) using radar and drifter values, respectively.

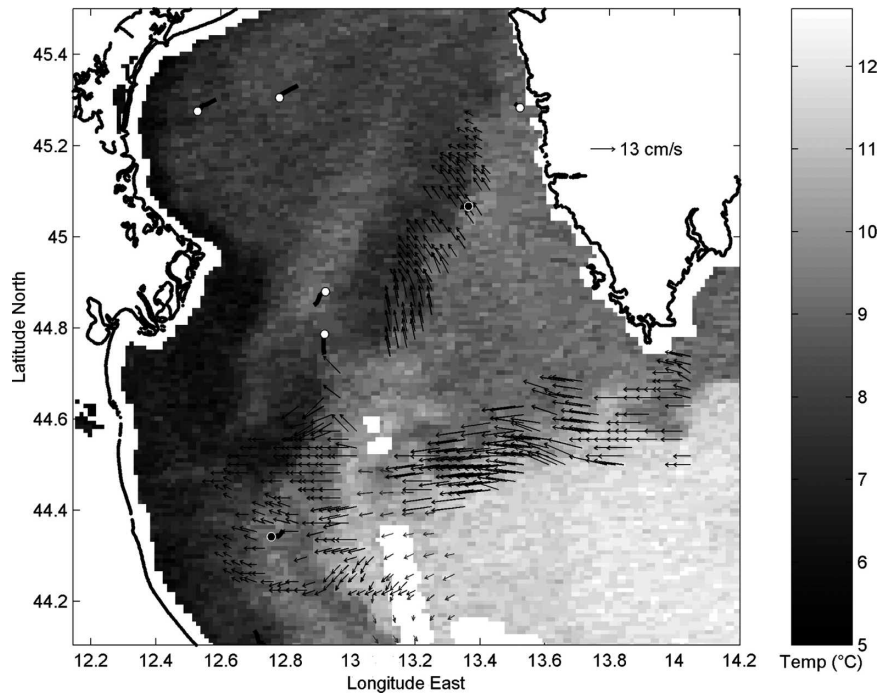


FIG. 8. Same as Fig. 2, but for 1311 UTC 23 Feb 2003 (NOAA-16).

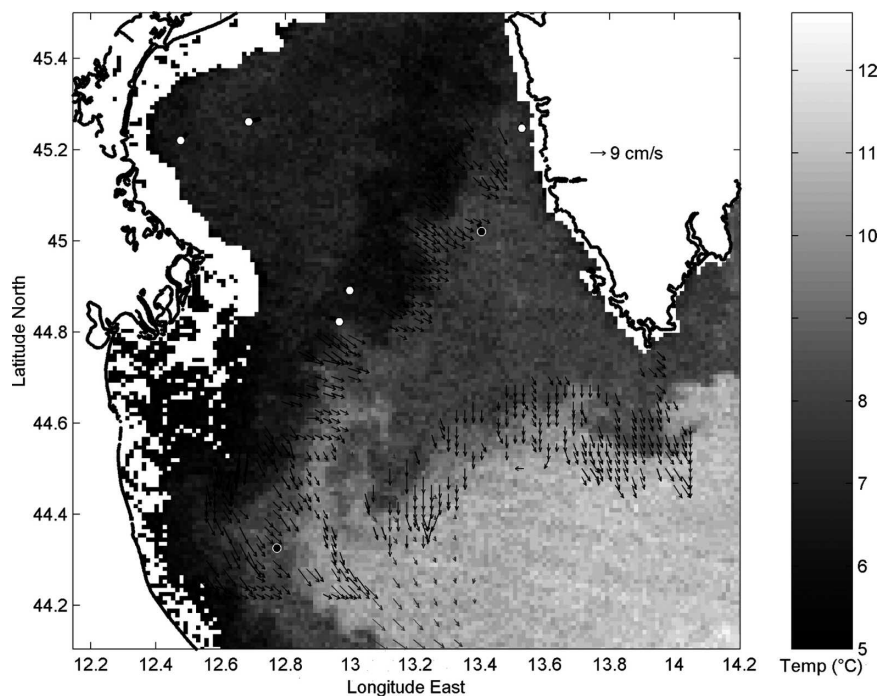


FIG. 9. Same as Fig. 2, but for 0124 UTC 25 Feb 2003 (NOAA-16).

#### b. Off the Monte Conero Promontory

We choose three pairs of images in July 2003 (Figs. 10–12) to describe the particular circulation pattern developed in the central Adriatic area off the Monte Conero Promontory (near Ancona).

The sequence of images on 17 July 2003 exhibits an unusual situation for the Italian side of the Adriatic Sea (Fig. 10). Indeed, the WAC has reversed its circulation pattern flowing northward due to a sustained southeasterly wind (sirocco) and a contemporary low discharge rate of the Po River, as reported by Poulain et al.

TABLE 2. Statistics of the surface velocity differences in the zonal ( $u$ ) and meridional ( $v$ ) directions for the comparison between MCC-derived and drifter data. The difference is defined as the drifter velocity minus the MCC estimate.

Pair of images	Figure No. corresponding to statistics	No. of vector pairs	Mean and standard deviation of velocity differences ( $\text{cm s}^{-1}$ )	
			$u$	$v$
7 Feb 2003 0457	4	1	-1.1	-7.3
7 Feb 2003 1249				
9 Feb 2003 1226	5	5	$-1.6 \pm 1.7$	$1.8 \pm 3.3$
9 Feb 2003 2032				
18 Feb 2003 1755	6	2	$-1.2 \pm 0.3$	$-4.9 \pm 2.2$
19 Feb 2003 0611				
20 Feb 2003 1601	7	6	$-1.4 \pm 3.1$	$-3.2 \pm 6.9$
21 Feb 2003 0208				
23 Feb 2003 1311	8	2	$5.7 \pm 4.3$	$-4.8 \pm 2$
24 Feb 2003 0135				
25 Feb 2003 0124	9	2	$-3.5 \pm 0.2$	$1.3 \pm 4.7$
25 Feb 2003 1249				
17 Jul 2003 0139	10	2	$-8.6 \pm 1.2$	$11 \pm 2.5$
17 Jul 2003 0953				
18 Jul 2003 0128	11	2	$3.3 \pm 9.6$	$-11.4 \pm 19$
18 Jul 2003 0930				
19 Jul 2003 1241	12	1	7.2	10.8
19 Jul 2003 2028				
Total	—	23	$-0.8 \pm 3.1$	$-1.1 \pm 5.9$

TABLE 3. Same as Table 2, but for radar data.

Pair of images	Figure No. corresponding to statistics	No. of vector pairs	Mean and standard deviation of velocity differences ( $\text{cm s}^{-1}$ )	
			$u$	$v$
25 Dec 2003 1255	2	11	$-9.6 \pm 2.8$	$-11.3 \pm 2.4$
25 Dec 2003 2032				
2 Feb 2003 1457	3	22	$3.1 \pm 3$	$-5 \pm 3$
2 Feb 2003 2130				
7 Feb 2003 0457	4	1	-1.3	-12.5
7 Feb 2003 1249				
9 Feb 2003 1226	5	7	$4.2 \pm 0.5$	$-2.5 \pm 0.6$
9 Feb 2003 2032				
18 Feb 2003 1755	6	10	$-3.8 \pm 3.8$	$-4.8 \pm 4.9$
19 Feb 2003 0611				
20 Feb 2003 1601	7	19	$-1.5 \pm 3.7$	$-6.2 \pm 1.9$
21 Feb 2003 0208				
23 Feb 2003 1311	8	9	$4.1 \pm 4.2$	$0.6 \pm 1.7$
24 Feb 2003 0135				
25 Feb 2003 0124	9	18	$1.9 \pm 1.9$	$6.2 \pm 2.6$
25 Feb 2003 1249				
Total	—	97	$0 \pm 1.6$	$-3.2 \pm 1.5$

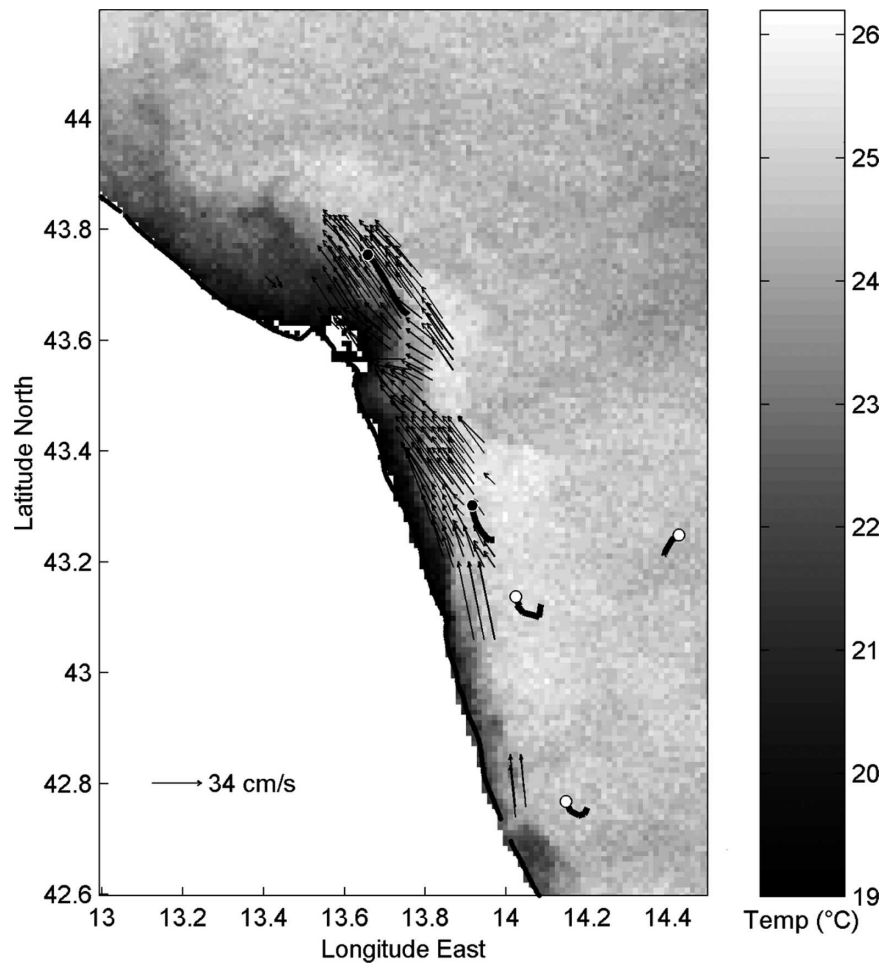


FIG. 10. Same as Fig. 2, but for 0139 UTC 17 Jul 2003 (NOAA-16).

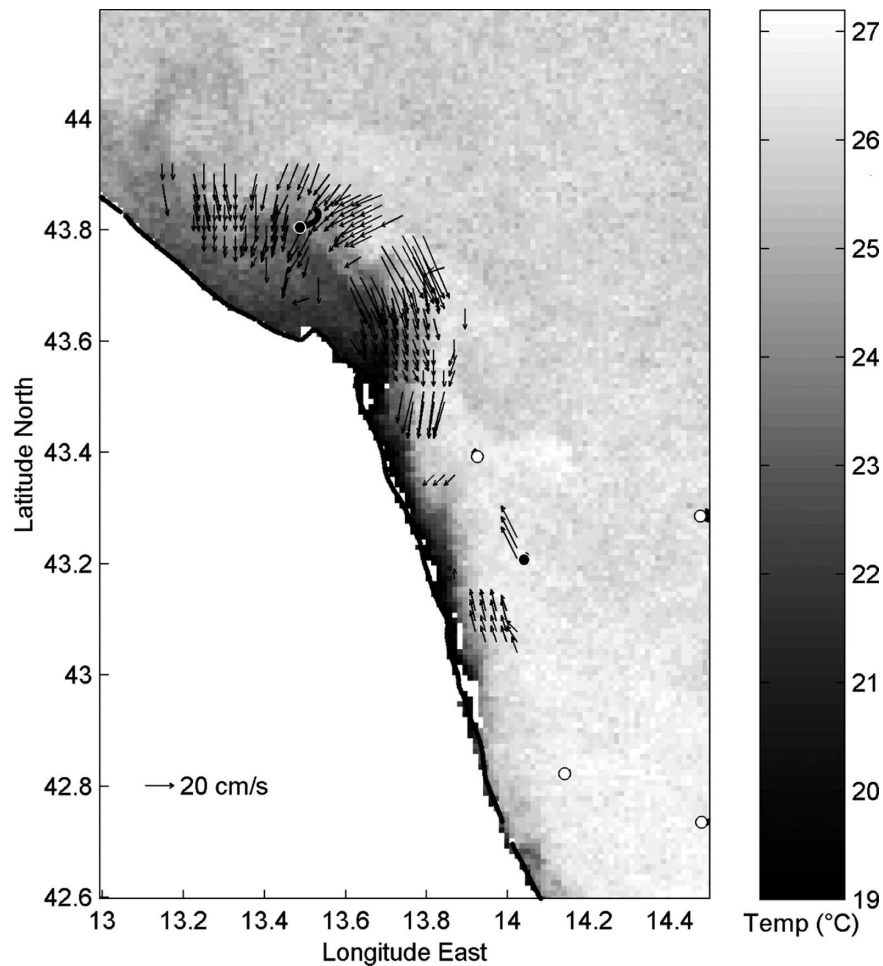


FIG. 11. Same as Fig. 2, but for 0128 UTC 18 Jul 2003 (NOAA-16).

(2004a). As a result, an exceptional upwelling event has developed off the Italian coast, bringing cold water to the surface separated by a strong horizontal thermal gradient from the warm open sea.

The MCC analysis reveals that the currents near the coast (in both relatively cold and warm waters) are northwestward and can have speeds reaching  $30\text{--}35\text{ cm s}^{-1}$  off the Monte Conero Promontory. These results are quite consistent with the drifter measurements. The pair on 17 July, even if the agreement between the MCC-derived and drifter velocities is the weakest, confirms that the MCC method estimates adequately the surface currents in terms of direction and speed in an area characterized by strong dynamic current reversal. North of the Promontory, the MCC currents are weaker and directed in the south and southwest (onshore) directions. They correspond to the cyclonic development of an instability feature protruding from the coastal cold zone (Poulain et al. 2004a).

In the second pair of images (Fig. 11) on 18 July the circulation pattern rotates cyclonically and the WAC starts to flow southward. The MCC vectors cross the thermal gradient features north of Ancona, as it is also clearly displayed by a collocated drifter. The pool of cold water is now moving in the south direction with a speed of  $15\text{--}20\text{ cm s}^{-1}$  according to both drifter measurements and MCC-derived values. The mean differences between the results obtained by the two techniques are  $3.3 \pm 9.6$  and  $-11.4 \pm 19\text{ cm s}^{-1}$  for the zonal and meridional components, respectively.

The last pair of images on 19 July reveals that the southward circulation along the Italian coast has been completely reestablished and the upwelling event is almost over (Fig. 12). Surface MCC-derived velocities over the cold pool off the Monte Conero Promontory are about  $20\text{ cm s}^{-1}$ , and a mean difference of 7.2 and  $10.8\text{ cm s}^{-1}$  for the zonal and meridional components, respectively, is found with respect to the drifter values.

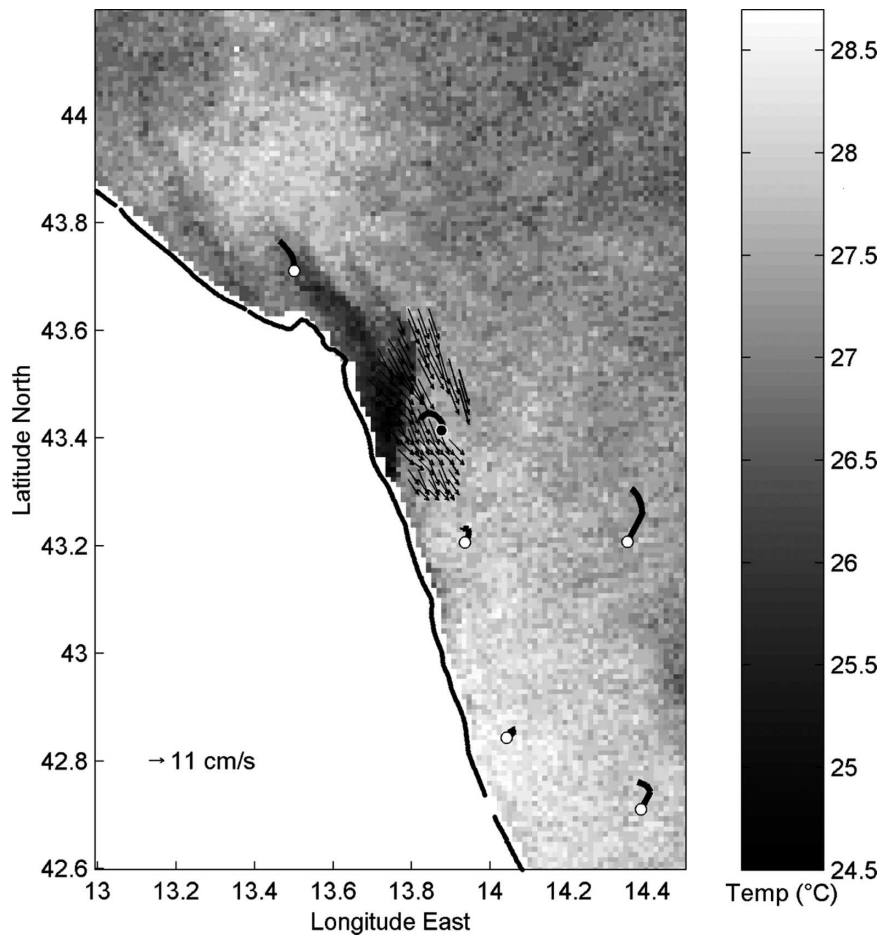


FIG. 12. Same as Fig. 2, but for 1241 UTC 19 Jul 2003 (NOAA-I6).

## 6. Discussion and conclusions

Sequential pairs of satellite SST images, produced from AVHRR data, were used to estimate surface currents in two areas of the Adriatic Sea. The MCC technique was applied to the image pairs using a  $25 \times 25$  pixel template window and a search window large enough to be able to track thermal features moving with a maximal speed of  $1 \text{ m s}^{-1}$ .

Filtering techniques were applied to the MCC-derived velocity vectors to discard results obtained by erroneous feature tracking. The various tests were efficient to remove erroneous MCC vectors and to produce accurate maps of the surface circulation in which the velocity and direction estimates are coherent over short distances (a few kilometers). In particular, the threshold of 0.8 for the minimum cross-correlation coefficient removes many erroneous vectors related to nonadvective processes that affect the SST patterns. The reciprocal technique was an essential and powerful filter to reject a large number of faulty vectors. The

nearest neighbor comparison was a useful method to filter velocity vectors that are spatially and artificially incoherent over a short distance. Finally, by discarding vectors whose distance from the location of the maximal temperature gradient is more than  $3/8$  of the template window diagonal, we guaranteed that the computed displacements corresponded to the thermal feature tracked. The final product of the filtering techniques is a selection of good MCC-derived vectors. Indeed, both the resulting velocity and direction estimates are spatially coherent in most of the thermal features. However, vectors appear less spatially coherent when the MCC analysis is computed with a window containing cloudy pixels (e.g., on 2 February 2003 in the northern Adriatic; Fig. 3).

Drifter position data were interpolated on the times of the images while HF coastal radar data were averaged over the time interval separating the images. A comparison was performed between the velocity components derived from the drifters and radars and those estimated by the MCC technique.

Our results show that surface MCC-derived velocities agree with the typical circulation pattern generally observed in the Adriatic basin. In general, MCC velocity estimates are quite consistent with collocated and cotemporal drifter and HF radar measurements, as was also reported by other authors (Afanasyev et al. 2002; Emery et al. 1986; Alberotanza and Zandonella 2004). On average, surface MCC-derived velocities are slightly overestimated with respect to the corresponding radar and drifter values: the zonal velocity component is larger by  $0.8 \pm 3.1 \text{ cm s}^{-1}$  with respect to the drifter measurements; the meridional velocity component is larger by  $3.2 \pm 1.5 \text{ cm s}^{-1}$  with respect to the radar measurements and by  $1.1 \pm 5.9 \text{ cm s}^{-1}$  with respect to the drifter measurements. The zonal velocity component is in good agreement with the radar results ( $0 \pm 1.6 \text{ cm s}^{-1}$ ). These differences are small considering that an image navigation error of 1 pixel produces an error of about  $3 \text{ cm s}^{-1}$ , using a time interval of 10 h, in the MCC velocity estimates. Considering each image pair, the largest mean values of the difference between radar (drifter) and MCC-derived velocity are  $-9.6 \pm 2.8$  and  $-11.3 \pm 2.4 \text{ cm s}^{-1}$  ( $-8.6 \pm 1.2$  and  $11 \pm 2.5 \text{ cm s}^{-1}$ ) for the zonal and meridional components, respectively. The corresponding smallest mean values, obtained from the difference between radar (drifter) and MCC-derived velocity, are  $4.1 \pm 4.2$  and  $0.6 \pm 1.7 \text{ cm s}^{-1}$  ( $-1.6 \pm 1.7$  and  $1.8 \pm 3.3 \text{ cm s}^{-1}$ ).

The relatively large discrepancy (as long as  $-11.4 \pm 19 \text{ cm s}^{-1}$ ) between MCC-derived and drifter velocity obtained for the pairs of images from 17 to 19 July (southern area of study) can be explained by considering that a drifter does not run along a straight line but follows the more complex pattern of the surface currents (including rotational motion), while vectors represent rectilinear translations. Moreover, the time separation between the images is 8 h and, during this lapse of time, some drifter trajectories appear rather twisted, although they display a general flow similar to the MCC vector estimates. Despite these problems, there is a good qualitative agreement between the MCC and the drifter displacements.

The application of the MCC technique in the Adriatic Sea presented in this paper is very successful for specific cases when strong thermal features can be tracked in sequences of satellite images. However, this method might not be adequate to monitor continuously (daily) the sea surface circulation since it requires several essential conditions (good image navigation, clear sky condition, and presence of thermal features) that are not generally satisfied simultaneously to produce reliable results.

Hence, it is encouraged that the MCC method in

marginal seas, such as the Adriatic, is used in conjunction with other techniques to estimate the sea surface circulation on a routine operational basis. For instance, a careful integration of MCC results with the data of HF radars and surface drifters could provide the best description of the surface currents. Care must be taken, however, when merging the different velocity datasets because of their varying specific natures (they might not correspond to measurements at exactly the same depths, they might represent averages on different time and space scales, etc.). All these datasets are generally “gappy” in both space and time and only their combination would yield velocity fields with extended geographical coverage at regular time intervals in a given sea area.

*Acknowledgments.* This research was supported by the Office of Naval Research under Contract N00140310291 as part of the DOLCEVITA program. The authors are grateful to L. Ursella and R. Barbanti for processing the drifter data, and to R. Gerin, C. Chavanne, and P. Flament for their help with the radar observations. The comments of the three anonymous reviewers contributed to improve the first version of the manuscript.

## REFERENCES

- Afanasyev, Y. D., A. G. Kostianoy, A. G. Zatsepin, and P.-M. Poulain, 2002: Analysis of velocity field in the eastern Black Sea from satellite data during the Black Sea '99 experiment. *J. Geophys. Res.*, **107**, 3098, doi:10.1029/2000JC000578.
- Alberotanza, L., and A. Zandonella, 2004: Surface current circulation estimation using NOAA/AVHRR images and comparison with HF radar current measurements. *Int. J. Remote Sens.*, **25**, 1357–1362.
- Barbanti, R., R. Lungwirth, and P.-M. Poulain, 2005: Stime dell'accuratezza del drifter tipo CODE con GPS nella determinazione della posizione geografica. OGS Tech. Rep. 32/2005/OGA/20, 16 pp.
- Barton, I. J., 2002: Ocean currents from successive satellite images: The reciprocal filtering technique. *J. Atmos. Oceanic Technol.*, **19**, 1677–1689.
- Borzelli, G., G. Manzella, S. Marullo, and R. Santoleri, 1999: Observations of coastal filaments in the Adriatic Sea. *J. Mar. Syst.*, **20**, 187–203.
- Bowen, M. M., W. J. Emery, J. L. Wilkin, T. C. Tildesley, I. J. Barton, and R. Knewton, 2002: Extracting multiyear surface currents from sequential thermal imagery using the maximum cross-correlation technique. *J. Atmos. Oceanic Technol.*, **19**, 1665–1676.
- Breaker, L. C., V. M. Krasnopolsky, D. B. Rao, and X.-H. Yan, 1994: The feasibility of estimating ocean surface currents on an operational basis using satellite feature tracking methods. *Bull. Amer. Meteor. Soc.*, **75**, 2085–2094.
- Chavanne, C., I. Janeković, P. Flament, P.-M. Poulain, M. Kuzmić, and K.-W. Gurgel, 2007: Tidal currents in the northwestern Adriatic Sea: High-frequency radio observations and

- numerical model predictions. *J. Geophys. Res.*, **112**, C03S21, doi:10.1029/2006JC003523.
- Collins, M. J., 1986: The estimation of pack-ice motion in digital satellite imagery by matched filtering. M.S. thesis, Dept. of Oceanography, University of British Columbia, 133 pp.
- , and W. J. Emery, 1988: A computational method for estimating sea ice motion in sequential SEASAT synthetic aperture radar imagery by matched filtering. *J. Geophys. Res.*, **93**, 9241–9251.
- Cushman-Roisin, B., M. Gacic, P.-M. Poulain, and A. Artegiani, Eds., 2001: *Physical Oceanography of the Adriatic Sea: Past, Present, and Future*. Kluwer Academic, 304 pp.
- Emery, W. J., A. C. Thomas, M. J. Collins, W. R. Crawford, and D. L. Mackas, 1986: An objective method for computing advective surface velocities from sequential infrared satellite images. *J. Geophys. Res.*, **91**, 12 865–12 878.
- , C. Fowler, J. Hawkins, and R. H. Preller, 1991: Fram Strait satellite image-derived ice motion. *J. Geophys. Res.*, **96**, 4751–4768.
- , —, and C. A. Clayson, 1992: Satellite-image-derived Gulf Stream currents compared with numerical model results. *J. Atmos. Oceanic Technol.*, **9**, 286–304.
- Hopkins, T. S., A. Artegiani, C. Kinder, and R. Pariente, 1999: A discussion of the northern Adriatic circulation and flushing as determined from the ELNA hydrography. The Adriatic Sea, European Commission Ecosystem Research Rep. 32, EUR 18834, 85–106.
- Kelly, K. A., and P. T. Strub, 1992: Comparison of velocity estimates from Advanced Very High Resolution Radiometer in the coastal transition zone. *J. Geophys. Res.*, **97**, 9653–9668.
- La Violette, P. E., 1984: The advection of submesoscale thermal features in the Alboran Sea Gyre. *J. Phys. Oceanogr.*, **14**, 450–505.
- Lee, C. M., and Coauthors, 2005: Northern Adriatic response to a wintertime bora wind event. *Eos, Trans. Amer. Geophys. Union*, **86**, 157–165.
- Leese, J. A., C. S. Novak, and B. B. Clarke, 1971: An automated technique for obtaining cloud motion from geosynchronous satellite data using cross-correlation. *J. Appl. Meteor.*, **10**, 110–132.
- Malanotte-Rizzoli, P., and A. Bergamasco, 1983: The dynamics of the coastal region of the northern Adriatic Sea. *J. Phys. Oceanogr.*, **13**, 1105–1130.
- McClain, E. P., W. Pichel, and C. Walton, 1985: Comparative performance of AVHRR-based multichannel sea surface temperatures. *J. Geophys. Res.*, **90**, 11 587–11 601.
- Ninnis, R. M., W. J. Emery, and M. J. Collins, 1986: Automated extraction of pack ice motion from Advanced Very High Resolution Radiometer imagery. *J. Geophys. Res.*, **91**, 10 725–10 734.
- Notarstefano, G., E. Mauri, and P.-M. Poulain, 2003: Trattamento dei dati AVHRR (Advanced Very High Resolution Radiometer) e produzione di immagini di SST (Sea Surface Temperature) con applicazione nel mare Adriatico. OGS Tech. Rep. 17/2003/OGA/09, 9 pp.
- , —, and —, 2006: Near-surface thermal structure and surface diurnal warming in the Adriatic Sea using satellite and drifter data. *Remote Sens. Environ.*, **101**, 194–211.
- Paduan, J. D., and H. C. Graber, 1997: Introduction to high-frequency radar: Reality and myth. *Oceanography*, **10**, 36–39.
- Poulain, P.-M., and R. Barbanti, 2003: DOLCEVITA-2 Cruise 26 May–15 June 2003: Report of drifter-related activities. OGS Tech. Rep. 29/2003/OGA/11, 17 pp.
- , L. Ursella, E. Mauri, and D. Deponte, 2003: DOLCEVITA-1 Cruise 31 January–24 February 2003: Report of drifter-related activities. OGS Tech. Rep. 08/2003/OGA/03, 32 pp.
- , E. Mauri, and L. Ursella, 2004a: Unusual upwelling event and current reversal off the Italian Adriatic coast in summer 2003. *Geophys. Res. Lett.*, **31**, L05303, doi:10.1029/2003GL019121.
- , R. Barbanti, R. Cecco, C. Fayos, E. Mauri, L. Ursella, and P. Zanasca, 2004b: Mediterranean surface drifter database: 2 June 1986 to 11 November 1999. OGS Tech. Rep. 78/2004/OGA/31, 17 pp.
- Svejkovsky, J., 1988: Sea surface flow estimation from Advanced Very High Resolution Radiometer and coastal zone color scanner satellite imagery: A verification study. *J. Geophys. Res.*, **93**, 6735–6743.
- Tokmakian, R., P. T. Strub, and J. McClean-Padman, 1990: Evaluation of the maximum cross-correlation method of estimating sea surface velocities from sequential satellite images. *J. Atmos. Oceanic Technol.*, **7**, 852–865.
- Ursella, L., R. Barbanti, and P.-M. Poulain, 2004: DOLCEVITA drifter program: Rapporto tecnico finale (in Italian). OGS Tech. Rep. 77/2004/OGA/30, 31 pp.
- , P.-M. Poulain, and R. P. Signell, 2006: Surface drifter derived circulation in the northern and middle Adriatic Sea: Response to wind regime and season. *J. Geophys. Res.*, **111**, C03S04, doi:10.1029/2005JC003177.
- Vastano, A. C., and S. E. Borders, 1984: Sea surface motion over an anticyclonic eddy on the Oyashio front. *Remote Sens. Environ.*, **16**, 87–90.
- , and R. O. Reid, 1985: Sea surface topography estimation with infrared satellite imagery. *J. Atmos. Oceanic Technol.*, **2**, 393–400.
- , S. E. Borders, and R. E. Wittemberg, 1985: Sea surface flow estimation with infrared and visible imagery. *J. Atmos. Oceanic Technol.*, **2**, 401–408.
- Wilkin, J. L., M. N. Bowen, and W. J. Emery, 2002: Mapping mesoscale currents by optimal interpolation of satellite radiometer and altimeter data. *Ocean Dyn.*, **52**, 95–103.